Perovskite Phases

International Edition: DOI: 10.1002/anie.201504396
German Edition: DOI: 10.1002/ange.201504396

An A-Site Mixed-Ammonium Solid Solution Perovskite Series of $[(NH_2NH_3)_x(CH_3NH_3)_{1-x}][Mn(HCOO)_3]$ ($x = 1.00$–0.67)

Sa Chen, Ran Shang, Bing-Wu Wang, Zhe-Ming Wang, and Song Gao**

Abstract: *The A-site mixed-ammonium solid solutions of metal–organic perovskites $[(NH_2NH_3)_x(CH_3NH_3)_{1-x}][Mn(HCOO)_3]$ ($x = 1.00$–0.67) exhibit para- to ferroelectric diffuse phase transitions with lowered transition temperatures from $x = 1.00$ to 0.67. These properties are due to the decreased framework distortion and polarization in their low temperature ferroelectric phases caused by the increased $CH_3NH_3^+$ concentration.*

The conventional electric and/or magnetic perovskite oxides ABO_3, such as ferroelectric $BaTiO_3$, antiferroelectric $PbZrO_3$,[1] and multiferroic $BiFeO_3$,[2] are of great importance in both fundamental science and technical application. The introduction of mixed metals to A- and/or B-sites has been widely used to control, modulate, or optimize the properties. For instance, the solid solution $PbZrO_3$–$PbTiO_3$ (PZT) with mixed zirconium and titanium components at the B-site shows exceptional piezoelectric properties,[1a] and the A-site La-doped PZT (PLZT) ceramics are transparent and exhibit interesting and useful electro-optic properties.[1b] For $BaTiO_3$, partially replacing the Ba atoms by Sr could lower the critical temperature (T_C) for application purposes.[1] The B-site mixed-metal perovskites of $Pb(Fe_{1/2}Nb_{1/2})O_3$ and $Pb(Fe_{2/3}W_{1/3})O_3$, and the A-site lanthanide (Ln) doped $(LnCa)MnO_3$ materials all exhibit multiferroic properties.[3]

Research on ammonium metal–formate frameworks (AMFFs) has recently attracted much attention because this class of metal–organic framework (MOF) materials exhibits interesting phase transitions, magnetic, dielectric, ferroelectric, and mechanic properties, and multiferroics,.[4–9] The perovskite AMFFs $[AH][M(HCOO)_3]$ or ABX_3 (where A = monoammonium AH^+, B = metal ion M, and X = $HCOO^-$) have been the primary compound types investigated.[4a,5a,6a,7c,8,10–16] These systems have a $4^{12}\cdot6^3$ metal–formate framework where the octahedral metal ions are linked by *anti–anti* formate ligands and the AH^+ cations are located within the cube-like cavities of the framework. Within these systems, the B-site metal ions are divalent 3d metal ions, Mg^{2+} ions, or mixed-metal ions,[16] such as Mn^{2+}/Zn^{2+}, Al^{3+}/Na^+, Fe^{3+}/Na^+, and Cr^{3+}/Na^+. For the A-site many ammonium species have been explored, such as $NH_2NH_3^+$,[10] $CH_3NH_3^+$,[11] $CH_3CH_2NH_3^+$,[11a] $(CH_3)_2NH_2^+$,[11a,12,13] $(CH_2)_3NH_2^+$,[14a] $C(NH_2)_3^+$,[14b] and $C_3N_2H_5^+$.[15] The use of different ammonium species has led to a wide range of dielectric, ferroelectric, mechanical, and dynamic properties and phase transition patterns, depending on the size, shape, and dynamics of the ammonium species and interactions between the ammonium and the framework. The A-site ammonium species thus acts as the key component of the perovskite AMFFs, similar to the role of the B-site metal ions in perovskite oxides. Therefore, it is important to investigate the effect of introducing mixed-ammonium species on the properties of the MOF-based perovskite materials. We herein report the first A-site solid solution perovskite series $[(NH_2NH_3)_x(CH_3NH_3)_{1-x}][Mn(HCOO)_3]$ ($x = 1.00$ to 0.67), incorporating the two ammonium species $NH_2NH_3^+$ (Hyz) and $CH_3NH_3^+$. $[NH_2NH_3][Mn(HCOO)_3]$ (100 Hyz) exhibits a ferro- to paraelectric transition from low temperature (LT) to high temperature (HT) at $T_C = 355$ K,[10] and the structure changes from a polar phase at LT to a nonpolar phase at HT. In contrast, $[CH_3NH_3][Mn(HCOO)_3]$ (0 Hyz) is nonpolar,[11] similar to the HT phase of 100 Hyz, and shows no phase transition. 100 Hyz differs from 0 Hyz by the difference of the NH_2 and CH_3 ends of the two ammonium species.[10] The compounds, 92 Hyz, 85 Hyz, 74 Hyz, and 67 Hyz (in which the number indicates the molar Hyz % within the material) display systematic changes in structure, phase-transition behavior, and dielectric properties upon variation of the Hyz %. Additionally, these compounds are weak ferromagnets and therefore may also be multiferroics.[4,5,8–10,12a,b] This series provides a new and interesting example in the currently very active research field of MOF-based solid solutions.[17]

The A-site mixed-ammonium solid solution compounds were prepared in methanol (see the experimental details in the Supporting Information). The crystalline materials showed homogeneous and uniform morphology (see Figure S1 in the Supporting Information) and the phase purity of the bulk samples was confirmed by elemental analysis, IR spectroscopy (Figure S2),[10,17b] and powder X-ray diffraction (PXRD) employing the Le Bail fitting method[17b,c,e,18] (Figures S3 and S4). The compounds were thermally stable up to 400 K (Figure S5). The DSC experiments (Figure S6) revealed that the phase transitions were reversible, and the T_C values decreased from 355 K for 100 Hyz[10] to 301 K for 67 Hyz (Figure 1, inset). Meanwhile, from 100 Hyz to 67 Hyz the DSC peaks became flatter and more thermally dispersed and the estimated ΔH, ΔS, and N values (where N is the ratio of state numbers in different phases) for the transitions decreased.

[*] S. Chen, R. Shang, Prof. B.-W. Wang, Prof. Z.-M. Wang, Prof. S. Gao
Beijing National Laboratory for Molecular Sciences
State Key Laboratory of Rare Earth Materials Chemistry and Applications, College of Chemistry and Molecular Engineering
Peking University, Beijing 100871 (China)
E-mail: zmw@pku.edu.cn
gaosong@pku.edu.cn

Supporting information for this article is available on the WWW under http://dx.doi.org/10.1002/anie.201504396.

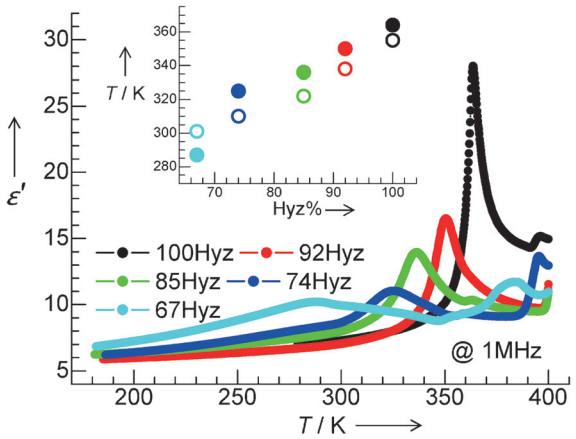

Figure 1. Dielectric constant (ε') plotted against T for compounds 100 Hyz, 92 Hyz, 85 Hyz, 74 Hyz, and 67 Hyz measured at 1 MHz. Inset: the T_C (filled circles; taken from DSC measurements) and T_P values (open circles; peak temperature in plots of ε' versus T) plotted against Hyz %.

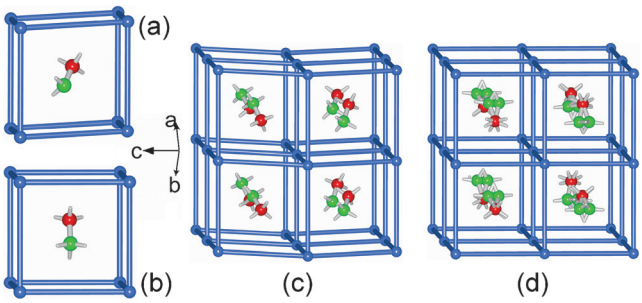

Figure 2. The cavities at 290 K in a) 100 Hyz and b) 0 Hyz and the structures of 85 Hyz showing the c) LT phase and d) HT phases. Color scheme: Mn = blue spheres, C/N atoms of the CH_3/NH_2 ends of ammonium = green, N of the NH_3 end of ammonium = red, H = white. $HCOO^-$ ligands are shown as blue sticks. The relationship between the LT and HT conventional cells is $a^{HT} \approx a^{LT}$, $b^{HT} \approx c^{LT}$, and $c^{HT} \approx -b^{LT}$, however in the text the LT lattice setting is always used.

The temperature-dependent dielectric permittivity parameters (ε' and $\tan\delta$; where $\tan\delta = \varepsilon''/\varepsilon'$, ε' = dielectric constant, ε'' = dielectric loss) for compounds 100 Hyz[10] to 67 Hyz are given in Figure 1 and Figure S7. At 1 MHz, the peak temperature/ε' value/FWHM (FWHM = full width at half maximum) are 364 K/28.0/9 K (100 Hyz), 350 K/16.5/15 K (92 Hyz), 336 K/14.0/23 K (85 Hyz), 325 K/11.0/30 K (74 Hyz), and 287 K/10.2/80 K (67 Hyz). The peak temperatures and peak broadenings are comparable to the observations in DSC runs (Figure S6). The dielectric peak broadening of 67 Hyz is more significant. The diffuse dielectric behaviors and the lowering of the T_C values with decreasing Hyz concentration are very similar to the behavior observed in the A-site solid solution oxides of $BaTiO_3$–$SrTiO_3$ and Sr–Ba niobates.[1] Applying Curie–Weiss laws to the ε' values recorded at 1 MHz on both HT and LT sides of the peak maximum (Figure S8) afforded C_{HT}/C_{LT} ratios of 1.7 to 2.3 (where C is the Curie constant), indicating that the phase transitions are second-order ferro- to paraelectric in nature.[1b,7d,10] Additional small anomalies are detected around 360 K in the ε' versus T traces for compounds 67 Hyz, 74 Hyz, 85 Hyz, and 92 Hyz at 1 MHz. On lowering the frequency (Figure S7) these anomalies become more significant, with ε' values rising to 30–40 at 1 kHz, higher than the ε' peak values at lower temperature. However, the compound 100 Hyz displays one dielectric anomaly at all frequencies.[10] For 100 Hyz to 67 Hyz, the $\tan\delta$ values are low until 350–360 K where they rise quickly, and the values are much larger at lower frequencies. Interestingly, the $\tan\delta$ versus temperature trace for compound 67 Hyz is somewhat frequency dependent.

The structures of all compounds in the series were determined at six different temperatures (Figure 2; Table S1, S2). The structures revealed that each compound undergoes the same type of phase transition[10] but with lowered T_C values from 100 Hyz to 67 Hyz, in good agreement with the results obtained by DSC and dielectric measurements. In contrast, compound 0 Hyz shows no phase transition between 180 and 400 K, confirmed by the determination of two structures at 350 K and 400 K and comparing them to the reported structures[11] at 180 K and 290 K and the DSC trace (Figure S6). For compounds 67 Hyz to 100 Hyz, the LT structures, in the polar space group $Pna2_1$, are ferroelectric. During the phase transition, the compounds change to HT paraelectric phases in the nonpolar space group $Pnma$. The transition is caused by the librational movement of the loosely H-bonded NH_2/CH_3 end of the $NH_2NH_3^+/CH_3NH_3^+$ ammonium pendulum in the cavities of the framework and related framework modulation and expansion (Figure 2; Figure S9). Such librational movement or disorder gives rise to a mirror plane within the structures, and the mirror plane is perpendicular to the c axis and runs through the C atoms of the $HCOO^-$ ligands extending in the c direction. The resulting mirror symmetry leads to the formation of centrosymmetric HT phases. 0 Hyz[11] has the same symmetry (space group $Pnma$ at both LT and HT) as the HT phases of 67 Hyz to 100 Hyz, with slightly larger lattice dimensions. The structure of 0 Hyz has larger b and c lattice constants but a smaller a constant, and the $CH_3NH_3^+$ ion is located on the mirror plane perpendicular to the c axis.

Several changes can be detected upon variation of temperature and $CH_3NH_3^+$ content, and these changes can be closely related to the phase transitions (Figure 3; Figure S9 and S10). From 100 Hyz to 67 Hyz, the b and c lattice constants and the cell volume expand but the a lattice parameter shrinks, giving rise to larger framework cavities to accommodate the ammonium ions of larger average size. The cube-like framework cavity (Figure 2 a, b), which has Mn ions at the apices, is not perfectly cubic. The lengths of Mn···Mn edges are the same to within 1 % (Table S2), so the distortion is mainly induced by the Mn-Mn-Mn angles. For the LT structures, the six faces of the cube-like cavity can be divided into three pairs, specifically top and bottom (tb), front and back (fb), and left and right (lr). The faces are slightly slanted, with two corner angles several degrees smaller than 90° and the other two larger than 90°. These angles are also the *cis* Mn-Mn-Mn angles within the $4^{12}\cdot6^3$ framework (Figure 2 c). The higher the $CH_3NH_3^+$ content, the closer to 90° are the *cis* angles. The *trans* Mn-Mn-Mn angle along the c axis is around 170° because the Mn centers in the c direction are not linearly aligned. At higher $CH_3NH_3^+$ concentrations this

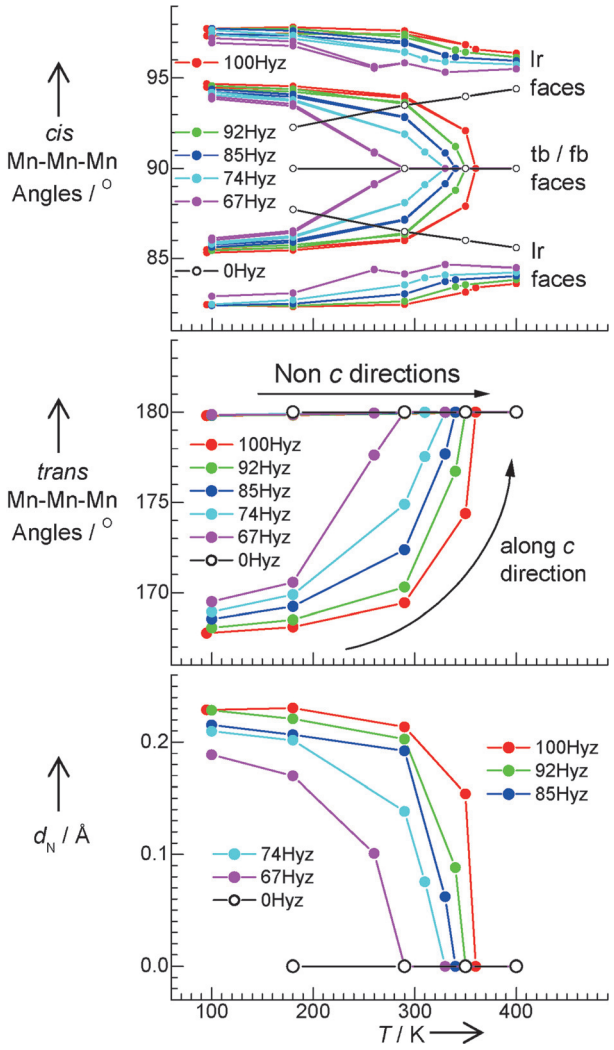

Figure 3. The temperature dependence of the *cis*/*trans* Mn-Mn-Mn angles and the d_N value. The left/right pair of faces is denoted by lr, top/bottom by tb, and front/back by fb.

angle is closer to 180°. The other two *trans* Mn-Mn-Mn angles are almost 180°. On warming, the Mn-Mn-Mn corner angles of the tb and fb faces approach and finally reach 90° in the HT phase (Figure 2d), but the lr faces are still slanted with angles measuring approximately 84/96°. Similarly, the *trans* Mn-Mn-Mn angle along the *c* direction gradually increases and finally reaches 180° in the HT phase. Another important parameter in the LT structures is the distance (d_N) of the NH_3^+ end of the cation deviating from the mirror plane which arises in the HT structure and is perpendicular to the *c* axis. The d_N value is thus the separation of the positive (cation) and negative (anionic framework) charges in the polar LT structures and represents the polarization of the LT ferroelectric phases.[7c,d,9b,c,10] The d_N value decreases upon heating and becomes zero after the phase transition. At higher $CH_3NH_3^+$ content, the d_N value is smaller. These structural variations clearly indicate that the introduction of the $CH_3NH_3^+$ cation at the A-site of 100 Hyz decreases the distortion of the framework and the polarization. Thus, the more symmetric HT structure and the phase transition are favored leading to lowered T_C, ΔS, N, and peak ε' values with increased $CH_3NH_3^+$ concentration. It is also noted that the cell parameters, obtained from single-crystal and powder diffractions (Figure S10), generally do not show linearity with ammonium composition (and do not follow Vegard's law[17b,c]), indicating the complicated packing effect of mixing the ammonium species in these solid-solution materials.

Two other interesting features in the dielectric responses for compounds 92 Hyz to 67 Hyz are the peak broadening for the ε' values, more significant for higher $CH_3NH_3^+$ content, and the second peaks or shoulders around 360 K, more prominent at lower frequencies. The peak broadening indicates that the phase transitions are diffuse, as reported previously in solid solution oxides.[1] It can be attributed to composition disorder[1b] or to the formation of clusters of the same cations in the lattice, with the cluster size and distribution depending on the ratio of the two cations, according to percolation theory.[19] Therefore, each material could be considered as a collection of microscopic regions having conventional dielectric and phase-transition behaviors but where the compositions vary from one to another. The macroscopic behavior is an envelope of the behaviors of the individual regions.[1b] The remarkable peak broadening for 67 Hyz is probably due to the fact that the $CH_3NH_3^+$ concentration is beyond the percolation limit of 31% for the simple cubic lattice.[11b,19] The detected gradual PXRD peak broadening (Figure S11) from 100 Hyz to 67 Hyz also suggested microscopic composition inhomogeneity.[17b] For the additional peaks or shoulders in the dielectric response, the temperatures are in fact very close to the peak temperature of 100 Hyz, but they are all above the individual T_C values. This is different from the conventional solid solution oxide materials.[1] A plausible explanation might be the damped oscillation of the ammonium pendulum above the T_C[7d,10] and should merit further investigation.

Finally, compounds 67 Hyz to 92 Hyz all display a long-range ordering of weak ferromagnetism around 8 K (Figure S12), very close to 100 Hyz[10] and 0 Hyz,[11] and comparable to other Mn-AMFFs.[5,12a,d,15] These materials show both ferroelectric and weak ferromagnetic orderings in the LT regions, suggesting that they may be interesting compounds in the study of MOF-based multiferroics.[4,5,8–10,12,20]

In conclusion, we have successfully synthesized A-site solid perovskite solutions of composition $[(NH_2NH_3)_x(CH_3NH_3)_{1-x}][Mn(HCOO)_3]$ ($x = 1.00$–0.67). Introducing $CH_3NH_3^+$ into $[NH_2NH_3][Mn(HCOO)_3]$ can decrease the framework distortion and the polarization of the LT phases resulting in more diffuse phase transitions with decreased T_C values, depending on the $CH_3NH_3^+$ concentration. This work demonstrates that the strategy of A-site modification can be successfully used in MOF-based perovskites, as in conventional perovskite oxides, to manipulate the phase transitions and related properties. It is anticipated that the study of A-site mixed-ammonium systems may become a popular research area, given the numerous possibilities to combine different ammonium species, such as $NH_2NH_3^+$ and $CH_3CH_2NH_3^+$, or $CH_3CH_2NH_3^+$ and $(CH_3)_2NH_2^+$. This work thus opens a new line of research into these MOF-based materials.

Acknowledgements

This work was supported by the NSFC (grant numbers 21171010, 21290170, 21290171, and 21321001) and the National Basic Research Program of China (grant number 2013CB933401). The authors thank Prof. Ying-Xia Wang and Dr. Jing Ju of Peking University for their kind help with PXRD and SEM studies.

Keywords: dielectric properties · manganese · metal–organic perovskites · phase transitions

How to cite: *Angew. Chem. Int. Ed.* **2015**, *54*, 11093–11096
Angew. Chem. **2015**, *127*, 11245–11248

[1] a) F. Jona, G. Shirane, *Ferroelectric Crystals*, Pergamon Press, Oxford, **1962**; b) M. E. Lines, A. M. Glass, *Principles and Applications of Ferroelectrics and Related Materials*, Clarendon Press, Oxford, **1977**.

[2] a) N. A. Spaldin, M. Fiebig, *Science* **2005**, *309*, 391 – 392; b) N. A. Spaldin, S. W. Cheong, R. Ramesh, *Phys. Today* **2010**, *63*, 38 – 43; c) D. I. Khomskii, *Physics* **2009**, *2*, 20.

[3] a) D. I. Khomskii, *J. Magn. Magn. Mater.* **2006**, *306*, 1 – 8; b) A. R. Akbashev, A. R. Kaul, *Russian Chem. Rev.* **2011**, *80*, 1159 – 1177.

[4] a) G. Kieslich, S. Sun, A. K. Cheetham, *Chem. Sci.* **2015**, *6*, 3430 – 3433; b) A. S. Tayi, A. Kaeser, M. Matsumoto, T. Aida, S. I. Stupp, *Nat. Chem.* **2015**, *7*, 281 – 294; c) W. Zhang, R.-G. Xiong, *Chem. Rev.* **2012**, *112*, 1163 – 1195; d) R. Ramesh, *Nature* **2009**, *461*, 1218 – 1219; e) A. K. Cheetham, C. N. R. Rao, *Science* **2007**, *318*, 58 – 59.

[5] a) R. Shang, S. Chen, Z. M. Wang, S. Gao in *Metal – Organic Framework Materials* (Eds.: L. R. Macgillivray, C. M. Lukehart), Wiley, Chichester, UK, **2014**; b) Z. M. Wang, K. L. Hu, S. Gao, H. Kobayashi, *Adv. Mater.* **2010**, *22*, 1526 – 1533.

[6] a) W. Li, A. Thirumurugan, P. T. Barton, Z. Lin, S. Henke, H. H.-M. Yeung, M. T. Wharmby, E. G. Bithell, C. J. Howard, A. K. Cheetham, *J. Am. Chem. Soc.* **2014**, *136*, 7801 – 7804; b) E. C. Spencer, M. S. R. N. Kiran, W. Li, U. Ramamurty, N. L. Ross, A. K. Cheetham, *Angew. Chem. Int. Ed.* **2014**, *53*, 5583 – 5586; *Angew. Chem.* **2014**, *126*, 5689 – 5692; c) W. Li, M. R. Probert, M. Kosa, T. D. Bennett, A. Thirumurugan, R. P. Burwood, M. Parinello, J. A. K. Howard, A. K. Cheetham, *J. Am. Chem. Soc.* **2012**, *134*, 11940 – 11943.

[7] a) R. Shang, Z. M. Wang, S. Gao, *Angew. Chem. Int. Ed.* **2015**, *54*, 2534 – 2537; *Angew. Chem.* **2015**, *127*, 2564 – 2567; b) R. Shang, S. Chen, K. L. Hu, Z. C. Jiang, B. W. Wang, M. Kurmoo, Z. M. Wang, S. Gao, *APL Mater.* **2014**, *2*, 124104; c) R. Shang, S. Chen, Z. M. Wang, S. Gao, *Chem. Eur. J.* **2014**, *20*, 15872 – 15883; d) R. Shang, G. C. Xu, Z. M. Wang, S. Gao, *Chem. Eur. J.* **2014**, *20*, 1146 – 1158.

[8] a) A. Stroppa, P. Jain, P. Barone, M. Marsman, J. M. Perez-Mato, A. K. Cheetham, H. W. Kroto, S. Picozzi, *Angew. Chem. Int. Ed.* **2011**, *50*, 5847 – 5850; *Angew. Chem.* **2011**, *123*, 5969 – 5972; b) A. Stroppa, P. Barone, P. Jain, J. M. Perez-Mato, S. Picozzi, *Adv. Mater.* **2013**, *25*, 2284 – 2290.

[9] a) L. Cañadillas-Delgado, O. Fabelo, J. A. Rodríguez-Velamazán, M. Lemée-Cailleau, S. A. Mason, E. Pardo, F. Lloret, J. Zhao, X. Bu, V. Simonet, C. V. Colin, J. Rodríguez-Carvajal, *J. Am. Chem. Soc.* **2012**, *134*, 19772 – 19781; b) G.-C. Xu, X.-M. Ma, L. Zhang, Z.-M. Wang, S. Gao, *J. Am. Chem. Soc.* **2010**, *132*, 9588 – 9590; c) G.-C. Xu, W. Zhang, X.-M. Ma, Y.-H. Chen, L. Zhang, H.-L. Cai, Z.-M. Wang, R.-G. Xiong, S. Gao, *J. Am. Chem. Soc.* **2011**, *133*, 14948 – 14951.

[10] S. Chen, R. Shang, K. L. Hu, Z. M. Wang, S. Gao, *Inorg. Chem. Front.* **2014**, *1*, 83 – 98.

[11] a) Z. M. Wang, B. Zhang, T. Otsuka, K. Inoue, H. Kobayashi, M. Kurmoo, *Dalton Trans.* **2004**, 2209 – 2216; b) R. Shang, X. Sun, Z.-M. Wang, S. Gao, *Chem. Asian J.* **2012**, *7*, 1697 – 1707.

[12] a) P. Jain, V. Ramachandran, R. J. Clark, H. D. Zhou, B. H. Toby, N. S. Dalal, H. W. Kroto, A. K. Cheetham, *J. Am. Chem. Soc.* **2009**, *131*, 13625 – 13627; b) D.-W. Fu, W. Zhang, H.-L. Cai, Y. Zhang, J.-Z. Ge, R.-G. Xiong, S. D. Huang, T. Nakamura, *Angew. Chem. Int. Ed.* **2011**, *50*, 11947 – 11951; *Angew. Chem.* **2011**, *123*, 12153 – 12157; c) M. Sánchez-Andújar, S. Presedo, S. Yáñez-Vilar, S. Castro-García, J. Shamir, M. A. Señarís-Rodríguez, *Inorg. Chem.* **2010**, *49*, 1510 – 1516; d) X.-Y. Wang, L. Gan, S.-W. Zhang, S. Gao, *Inorg. Chem.* **2004**, *43*, 4615 – 4625.

[13] a) R. I. Thomson, P. Jain, A. K. Cheetham, M. A. Carpenter, *Phys. Rev. B* **2012**, *86*, 214304; b) T. Besara, P. Jain, N. S. Dalal, P. L. Kuhns, A. P. Reyes, H. W. Kroto, A. K. Cheetham, *Proc. Natl. Acad. Sci. USA* **2011**, *108*, 6828 – 6832; c) T. Asaji, K. Ashitomi, *J. Phys. Chem. C* **2013**, *117*, 10185 – 10190; d) J.-C. Tan, P. Jain, A. K. Cheetham, *Dalton Trans.* **2012**, *41*, 3949 – 3952.

[14] a) B. Zhou, Y. Imai, A. Kobayashi, Z.-M. Wang, H. Kobayashi, *Angew. Chem. Int. Ed.* **2011**, *50*, 11441 – 11445; *Angew. Chem.* **2011**, *123*, 11643 – 11647; b) K.-L. Hu, M. Kurmoo, Z.-M. Wang, S. Gao, *Chem. Eur. J.* **2009**, *15*, 12050 – 12064.

[15] B. Pato-Doldán, L. C. Gómez-Aguirre, J. M. Bermúdez-García, M. Sánchez-Andújar, A. Fondado, J. Mira, S. Castro-García, M. A. Señarís-Rodríguez, *RSC Adv.* **2013**, *3*, 22404 – 22411.

[16] a) M. Mączka, A. Pietraszko, L. Macalik, A. Sieradzki, J. Trzmielb, A. Pikula, *Dalton Trans.* **2014**, *43*, 17075 – 17084; b) A. Plutecka, U. Rychlewska, *Acta Crystallogr. Sect. C* **2009**, *65*, m75 – m77; c) M. Mączka, B. Bondzior, P. Dereń, A. Sieradzki, J. Trzmiel, A. Pietraszkoa, J. Hanuza, *Dalton Trans.* **2015**, *44*, 6871 – 6879.

[17] a) H. Furukawa, U. Müller, O. M. Yaghi, *Angew. Chem. Int. Ed.* **2015**, *54*, 3417 – 3430; *Angew. Chem.* **2015**, *127*, 3480 – 3494; b) H. H.-M. Yeung, W. Li, P. J. Saines, T. K. J. Köster, C. P. Grey, A. K. Cheetham, *Angew. Chem. Int. Ed.* **2013**, *52*, 5544 – 5547; *Angew. Chem.* **2013**, *125*, 5654 – 5657; c) T. Fukushima, S. Horike, H. Kobayashi, M. Tsujimoto, S. Isoda, M. L. Foo, Y. Kubota, M. Takata, S. Kitagawa, *J. Am. Chem. Soc.* **2012**, *134*, 13341 – 13347; d) H. Deng, C. J. Doonan, H. Furukawa, R. B. Ferreira, J. Towne, C. B. Knobler, B. Wang, O. M. Yaghi, *Science* **2010**, *327*, 846 – 850; e) T. Fukushima, S. Horike, Y. Inubushi, K. Nakagawa, Y. Kubota, M. Takata, S. Kitagawa, *Angew. Chem. Int. Ed.* **2010**, *49*, 4820 – 4824; *Angew. Chem.* **2010**, *122*, 4930 – 4934.

[18] W. I. F. David, D. S. Sivia in *Structure Determination from Powder Diffraction Data* (Eds.: W. I. F. David, K. Shankland, L. B. McCusker, C. Baerlocher), Oxford University Press, Oxford, **2002**, pp. 138 – 143.

[19] a) K. Christensen, N. R. Moloney, *Complexity and Criticality*, Imperial College Press, London, **2005**; b) R. B. Stinchcombe, *J. Phys. C: Solid State Phys.* **1979**, *12*, 4533 – 4552.

[20] a) E. Pardo, C. Train, H. Liu, L. M. Chamoreau, B. Dkhil, K. Boubekeur, F. Lloret, K. Nakatani, H. Tokoro, S. i. Ohkoshi, M. Verdaguer, *Angew. Chem. Int. Ed.* **2012**, *51*, 8356 – 8360; *Angew. Chem.* **2012**, *124*, 8481 – 8485; b) S. i. Ohkoshi, H. Tokoro, T. Matsuda, H. Takahashi, H. Irie, K. Hashimoto, *Angew. Chem. Int. Ed.* **2007**, *46*, 3238 – 3241; *Angew. Chem.* **2007**, *119*, 3302 – 3305; c) H. B. Cui, Z. M. Wang, K. Takahashi, Y. Okano, H. Kobayashi, A. Kobayashi, *J. Am. Chem. Soc.* **2006**, *128*, 15074 – 15075.

Received: May 14, 2015
Revised: June 25, 2015
Published online: August 4, 2015

